A Two-Dimensional (2D) Analytical Model for the Potential Distribution and Threshold Voltage of Short-Channel Ion-Implanted GaAs MESFETs under Dark and Illuminated Conditions

Shweta Tripathi and S. Jit

Abstract—**A two-dimensional (2D) analytical model for the potential distribution and threshold voltage of short-channel ion-implanted GaAs MESFETs operating in the sub-threshold regime has been presented. A double-integrable Gaussian-like function has been assumed as the doping distribution profile in the vertical direction of the channel. The Schottky gate has been assumed to be semi-transparent through which optical radiation is coupled into the device. The 2D potential distribution in the channel of the short-channel device has been obtained by solving the 2D Poisson's equation by using suitable boundary conditions. The effects of excess carrier generation due to the incident optical radiation in channel region have been included in the Poisson's equation to study the optical effects on the device. The potential function has been utilized to model the threshold voltage of the device under dark and illuminated conditions. The proposed model has been verified by comparing the theoretically predicted results with simulated data obtained by using the commercially available ATLAS^{TM} 2D device simulator.**

Index Terms—**Optically controlled GaAs MESFET, optical biasing, ion implantation, gaussian doping profile, threshold voltage, MMIC, Poisson's equation**

Manuscript received Nov. 29, 2010; revised Jan. 24, 2011.
Centre for Research in Microelectronics (CRME), Department of Electronics Engineering, Institute of Technology, Banaras Hindu University, Varanasi-221005, India
E-mail : sjit.ece@itbhu.ac.in

I. INTRODUCTION

GaAs Metal-Semiconductor Field Effect Transistors (GaAs MESFETs) have drawn considerable attention for the designing of high-speed digital/analog integrated circuits and microwave monolithic ICs [1-9]. A number of studies have illustrated that both the dc and microwave characteristics of a GaAs MESFET can be modified by coupling a fraction of the optical power radiated by an external source into the channel of the device [10-17]. The excess electron-hole pair generation due to the optical radiation in the channel is utilized to control the device characteristics. Since these excess electron-hole pairs can be controlled by the radiated power level of the external optical source, the radiated power level has direct control on the device characteristics. The optical radiation incident on the device can thus be viewed as an extra input terminal of the MESFET through which the microwave device or circuit (e.g. MMIC) performance can be governed. A MESFET with a transparent or semi-transparent Schottky-metal (at the gate) to the desired incident radiation is known as optically controlled field effect transistor (OPFET).

Optically controlled microwave devices and systems exhibit certain advantages such as size reduction, signal isolation, large bandwidth and immunity to electromagnetic interference. It has also been shown that the incident illumination reduces the noise figure but increases the unilateral power gain of a GaAs OPFET [18-19]. Due to such properties, high-speed, low-cost, monolithically

integrated optically gated GaAs MESFETs are presently in high demand for low-wavelength high-frequency optical communication systems [10, 12]. A number of investigations [20-25] have previously been performed to study the photo effects on GaAs-MESFET to describe its operation and application under dark and illuminated conditions. GaAs MESFETs with gate length values in the range of 0.2-0.5 μm show high drain-source current and large transconductance values at microwave frequencies [26]. The one dimensional (1D) Poisson's equation will fail to provide potential distribution of such MESFETs with a channel length in the above mentioned range since the electrical characteristics of these scaled-down devices are known to be greatly influenced by the two-dimensional potential distribution and high electric field effects [27]. Thus, the 2D Poisson's equation is required to be solved to obtain the channel potential and threshold voltage of short-channel devices which can be utilized for further modeling of the electrical characteristics of the device.

A number of studies have [28-29] demonstrated that shortening of channel length leads to small-geometry transistors for denser as well as faster integrated circuits; and non uniform heavy doping in the channel region can provide higher drain saturation current and transconductance. In general, various techniques can be used for producing non-uniform doping in the channel region of the device among which ion-implantation is found to be very effective for improved GaAs MESFET performance [30]. It may be mentioned that the ion-implantation method produces a Gaussian doping profile which is an analytically non-integrable function. In other words, integration of the Gaussian function within finite limits introduces the error function which is not analytical in nature. Thus, the 2D modeling of the potential distribution and threshold voltage of short-channel ion-implanted GaAs MESFETs is always a difficult and challenging task. The complexity is increased further if the modeling is carried out for a short-gate length GaAs MESFETs operating under illuminated condition where the additional effects of incident illumination on the device characteristics is required to be included in the model. Bose et al [25] presented the modeling of short channel GaAs MESFETs under illuminated condition. However, they assumed uniformly distributed device channel and results presented by them are not validated by any experimental or numerical simulation data. To the best of our knowledge, no work has been reported so far in the literature for the two-dimensional analytical model of an ion-implanted short-channel GaAs MESFETs under dark and illuminations.

In the present paper, an attempt has been made to analytically model the channel potential and threshold voltage of short channel optically biased GaAs MESFETs with vertical Gaussian profile to achieve faster and denser components for photonic MMICs. The model uses a Gaussian-like analytic function proposed by Dasgupta et al [31] in place of the actual non-analytic Gaussian function for making the model purely analytical one. The model is simplified further by assuming that the vertical channel doping is Gaussian in nature whereas it is uniform in the lateral direction. The 2D potential distribution function is obtained by solving the 2D Poisson's equation using superposition method in conjunction with appropriate boundary conditions. Appropriate modification has been incorporated in the Poisson's equation to include the photo effects on the device characteristics of the GaAs MESFETs under illuminated condition. Since the threshold voltage is the key parameter in both the dc and microwave circuit design using GaAs MESFETs, the effect of optical illumination on threshold voltage of GaAs OPFET has also been investigated. Theoretically predicted results are compared with the simulation data obtained from ATLAS^{TM}, a commercially available 2D device simulator [32].

II. DEVICE DETAILS

The schematic structure of fully depleted optically biased GaAs MESFET used for modeling is shown in Fig. 1 where, a and L are active layer thickness and gate length respectively. The substrate of the device is assumed to be an undoped high pure LEC (Liquid-Encapsulated Czochralski) semi-insulating GaAs material. The active channel region of the device is an n-GaAs layer which can be obtained by ion implanting Si into semi-insulating substrate. Monochromatic light of energy greater than or equal to the band gap energy of GaAs is allowed to fall upon the gate area of the device along the y-axis. Indium Tin Oxide (ITO) has been used as the Schottky-gate metal due to its high optical trans-mittance

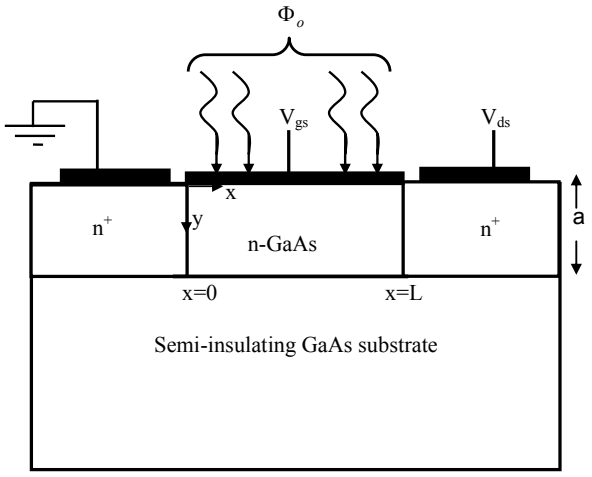

Fig. 1. Schematic diagram of the GaAs MESFET where L, a, V_{gs}, V_{ds} and Φ_0 are the channel length, channel thickness, gate to source voltage, drain to source voltage and photon density of the illumination respectively.

of incident illumination on its gate surface [33].

The undoped substrate is assumed to have a uniform doping concentration of N_s. The implantation is assumed from an infinitesimal beam that scanned uniformly across the substrate surface so that the ion distribution profile becomes 1D Gaussian function described by [34]

$$N(y)=\frac{Q}{\sigma\sqrt{2\pi}}e^{\left[-\left(\frac{y-R_p}{\sigma\sqrt{2}}\right)^2\right]}=N_p\,e^{\left[-\left(\frac{y-R_p}{\sigma\sqrt{2}}\right)^2\right]} \quad (1)$$

where Q is the dose, R_p is the projected range, σ is the projected straggle, and $N_p=\frac{Q}{\sigma\sqrt{2\pi}}$ is peak ion concentration in the substrate.

Taking the substrate doping concentration N_s into account, the doping distribution in the channel can approximately be described by [35]

$$N_d(y)=N_s+(N_p-N_s)\,e^{\left[-\left(\frac{y-R_p}{\sigma\sqrt{2}}\right)^2\right]}=N_s+(N_p-N_s)F(y) \quad (2)$$

where

$$F(y)=e^{\left[-\left(\frac{y-R_p}{\sigma\sqrt{2}}\right)^2\right]} \quad (3)$$

Note that $N_d(y)$ is an analytically non-integrable function of y because of the exponential function $F(y)$. To remove this difficulty, we have used an approximate analytic form of $F(y)$ as [31]

$$F(y)\approx c_c\left[\left\{a_c+\frac{2b_c\beta}{\sqrt{2}\,\sigma}(y-R_p)\right\}^2-2b_c\right]e^{\left[-\left\{\frac{a_c\beta}{\sqrt{2}\sigma}(y-R_p)+\frac{b_c}{2\sigma^2}(y-R_p)^2\right\}\right]} \quad (4)$$

where

$a_c=1.7857142$, $b_c=0.6460835$, $c_c=0.28\sqrt{\pi}$ and

$$\beta=\begin{cases}+1 & \text{for } y>R_p\\ -1 & \text{for } y<R_p\end{cases}$$

The channel region of the device is considered to be a fully depleted one and electron-hole pairs are generated due to the incident optical radiation in the depletion region below the semi-transparent Schottky gate. The photo-generated holes are swept out into the metal side through the gate-channel junction due to the presence of the static electric field in the depletion region. This results in a photocurrent flowing from the active layer of the MESFET to the metal at the gate and consequently develops a photovoltage V_{op} at the Schottky junction, which makes the junction forward biased.

III. THEORETICAL MODEL

1. Modeling of the 2D Channel Potential Function

Let $\phi(x,y)$ be the 2D potential distribution of the channel. Now, $\phi(x,y)$ can be determined by solving the following 2D Poisson's equation in the fully depleted rectangular channel region:

$$\frac{d^2\phi(x,y)}{dx^2}+\frac{d^2\phi(x,y)}{dy^2}=-\frac{qN_D(y)}{\varepsilon_s} \quad (5)$$

where ε_s is the dielectric permittivity of GaAs semiconductor, q is electron charge and $N_D(y)$ is the net doping concentration in the active channel region

under illuminated condition which can be expressed as [25]

$$N_D(y) = N_d(y) + G(y)\tau_n - \frac{R\tau_p}{a} \tag{6}$$

where $N_d(y)$ represents the doping profile defined by Eq. (2). R is the surface recombination rate, α is the absorption coefficient of GaAs material, τ_n and τ_p are the life time of electrons and holes, respectively and $G(y)$ is the photo-generation rate given by [34]

$$G(y) = \Phi_0 \alpha e^{(-\alpha y)} \tag{7}$$

where Φ_0 is the photon flux density expressed as

$$\Phi_0 = \frac{P_{in} T_m}{h\upsilon ZL} \tag{8}$$

where P_{in} is the incident optical power, Z is the width of the gate-metal, L is the gate length, T_m is the optical transmission coefficient for the gate metal, h is Planck's constant and υ is the frequency of the incident light.

We can use the following boundary conditions [36] for solving Eq. (5):

$$\phi(x,0) = V_{bi} - V_{gs} - V_{op} \tag{9}$$

$$\phi(0,y) = V_{bi} \tag{10}$$

$$\phi(L,y) = V_{bi} + V_{ds} \tag{11}$$

$$\left.\frac{\partial \phi(x,y)}{\partial y}\right|_{y=a} = 0 \tag{12}$$

where V_{bi} is the Schottky-barrier built-in potential, V_{gs} is the applied gate bias and V_{op} is the photo-voltage developed at the Schottky junction due to illumination which can be described by [37]

$$V_{op} = \frac{nkT}{q} \ln\left(1 + \frac{J_p(0)}{J_s}\right) \tag{13}$$

where J_s is reverse saturation current density at the gate depletion layer interface, k is the Boltzman constant, T is room temperature(i.e., 300 K), n is the ideality factor of Schottky junction, q is the charge of an electron, and $J_p(0)$ is the hole current density crossing the gate-channel interface given by [37]

$$J_p(0) = q v_p p_d(y)\big|_{y=0} \tag{14}$$

where v_p is the saturation velocity of hole and $P_d(y)$ is the photo-generated hole density in the depletion region and $p_d(y)\big|_{y=0}$ is described by [37]

$$p_d(y)\big|_{y=0} = \left(\frac{\Phi_o \alpha \tau_p}{1 - \alpha \tau_p v_p}\right)\left[1 - e^{(-\alpha a)}\right] \tag{15}$$

Applying the superposition technique [38] to solve the 2D Poisson's equation described by Eq. (5), $\phi(x,y)$ can be expressed as

$$\phi(x,y) = \varphi_{1D}(y) + \varphi_{2D}(x,y) \tag{16}$$

where, $\varphi_{1D}(y)$ is 1D potential function of the long-channel MESFETs and $\varphi_{2D}(x,y)$ is the 2D potential function responsible for the short channel effects.

The long-channel potential function $\varphi_{1D}(y)$ can be obtained by solving following 1D Poisson's equation

$$\frac{d^2 \varphi_{1D}(y)}{dx^2} = -\frac{qN_D(y)}{\varepsilon_s} \tag{17}$$

with the following boundary conditions:

$$\varphi_{1D}(y)\big|_{y=0} = V_{bi} - V_{gs} - V_{op} \tag{18}$$

$$\left.\frac{\partial \varphi_{1D}(y)}{\partial y}\right|_{y=a} = 0 \tag{19}$$

The function $\varphi_{1D}(y)$ can be obtained by integrating Eq. (17) twice and can be written as

$$\varphi_{1D}(y)=\frac{q\left(\sigma\sqrt{2}\right)^2}{\varepsilon_s}\Bigg[c_c\left(N_p-N_s\right)e^{\left[-\left(a_c\left(\frac{y-R_p}{\sqrt{2}\sigma}\right)+b_c\left(\frac{y-R_p}{\sqrt{2}\sigma}\right)^2\right)\right]}-\frac{R\tau_p}{a}\left(\frac{y-R_p}{\sqrt{2}\sigma}\right)^2+\frac{\Phi_o\tau_n e^{\left(-\alpha R_p\right)}e^{\left(-\alpha\left(y-R_p\right)\right)}}{\alpha^2\left(\sigma\sqrt{2}\right)^2}+\frac{N_s}{2}\left(\frac{y-R_p}{\sqrt{2}\sigma}\right)^2+A\left(\frac{y-R_p}{\sqrt{2}\sigma}\right)+B\Bigg] \quad (20)$$

where A, B are the arbitrary constants expressed as

$$A=-\frac{q\sigma\sqrt{2}}{\varepsilon_s}\Bigg[-c_c\left(N_p-N_s\right)\left(a_c+2b_c\left(\frac{a-R_p}{\sqrt{2}\sigma}\right)\right)\times e^{\left[-\left(a_c\left(\frac{a-R_p}{\sqrt{2}\sigma}\right)+b_c\left(\frac{a-R_p}{\sqrt{2}\sigma}\right)^2\right)\right]}+N_s\left(\frac{a-R_p}{\sqrt{2}\sigma}\right)-\frac{R\tau_p}{a}\left(\frac{a-R_p}{\sqrt{2}\sigma}\right)-\frac{\left(\Phi_o\tau_n e^{\left(-\alpha R_p\right)}e^{\left(-\alpha\left(a-R_p\right)\right)}\right)}{\alpha\sigma\sqrt{2}}\Bigg] \quad (21)$$

$$B=-\Bigg[c_c\left(N_p-N_s\right)e^{\left[-\left(a_c\left(\frac{-R_p}{\sqrt{2}\sigma}\right)+b_c\left(\frac{-R_p}{\sqrt{2}\sigma}\right)^2\right)\right]}+\frac{N_s}{4}\left(\frac{-R_p}{\sigma}\right)^2-\frac{R\tau_p}{2a}\left(\frac{-R_p}{\sigma}\right)^2+\frac{\Phi_o\tau_n e^{\left(-\alpha R_p\right)}e^{\left(\alpha R_p\right)}}{\alpha^2\left(\sigma\sqrt{2}\right)^2}+A\left(\frac{-R_p}{\sqrt{2}\sigma}\right)-\frac{\varepsilon_s\left(V_{bi}-V_{gs}-V_{op}\right)}{q\left(\sigma\sqrt{2}\right)^2}\Bigg] \quad (22)$$

Now, the $\varphi_{2D}(x,y)$ can be obtained by the 2D Laplace's equation

$$\frac{\partial^2\varphi_{2D}(x,y)}{\partial x^2}+\frac{\partial^2\varphi_{2D}(x,y)}{\partial y^2}=0 \quad (23)$$

By using the following boundary conditions derived from Eqs.(9)-(12) in conjunction with Eq.(18)-(19)

$$\varphi_{2D}(x,0)=0 \quad (24)$$

$$\varphi_{2D}(0,y)=V_{bi}-\varphi_{1D}(y) \quad (25)$$

$$\varphi_{2D}(L,y)=V_{bi}+V_{ds}-\varphi_{1D}(y) \quad (26)$$

$$\left.\frac{d\varphi_{2D}(x,y)}{dy}\right|_{y=a}=0 \quad (27)$$

Applying the standard technique of separation of variables [39] and using the boundary conditions described by Eqs. (24-27), $\varphi_{2D}(x,y)$ can be expressed as

$$\varphi_{2D}(x,y)=\sum_{n=1}^{\infty}\frac{\sin(k_n y)}{\sinh(k_n L)}\left\{A_n\sinh[k_n(L-x)]+B_n\sinh(k_n x)\right\} \quad (28)$$

where

$$k_n=\frac{(2n+1)\pi}{2a} \quad (29)$$

$$A_n=\frac{C_{1n}-C_{2n}-C_{3n}+C_{4n}-C_{5n}+C_{6n}+C_{7n}}{M_n} \quad (30)$$

$$B_n=\frac{C_{1n}+C_{11n}-C_{2n}-C_{3n}+C_{4n}-C_{5n}+C_{6n}+C_{7n}}{M_n} \quad (31)$$

$$C_{1n}=-\frac{q\left(\sigma\sqrt{2}\right)^3 c_c(N_p-N_s)}{\varepsilon_s{}^1k_n^3}\Big[2b_c+k_n^2+\left(-2b_c+\left(-1+a\left(a_c+b_c a\right)\right)k_n^2\cos\left(k_n a\right)-\left(a_c+2b_c a\right)k_n\right)\sin\left(k_n a\right)\Big] \quad (32)$$

$$C_{11n}=\frac{V_{ds}}{k_n}-\frac{V_{ds}\cos k_n a}{k_n} \quad (33)$$

$$C_{2n}=\frac{q\left(\sigma\sqrt{2}\right)^3 N_s}{2\varepsilon_s k_n^3}\left[-2+\left(2-a^2k_n^2\right)\cos\left(ak_n\right)+2ak_n\cos\left(ak_n\right)\right] \quad (34)$$

$$C_{3n}=\frac{q\left(\sigma\sqrt{2}\right)\Phi_o\tau_n}{\alpha}e^{\left(-\alpha R_p-\alpha\sigma\sqrt{2}a\right)}\times\left[\frac{k_n e^{\left(\alpha\sigma\sqrt{2}a\right)}-k_n\cos\left(ak_n\right)-\alpha\sigma\sqrt{2}\sin\left(ak_n\right)}{\alpha\left(\sigma\sqrt{2}\right)^2+k_n^2}\right]-\left(\frac{V_{bi}}{k_n}-\frac{V_{bi}\cos k_n a}{k_n}\right) \quad (35)$$

$$C_{4n}=\frac{q\left(\sigma\sqrt{2}\right)^3 R\tau_p}{2a\varepsilon_s k_n^3}\left[-2+\left(2-a^2k_n^2\right)\cos\left(ak_n\right)+2ak_n\cos\left(ak_n\right)\right] \quad (36)$$

$$C_{5n}=\frac{Aq^2\left(\sigma\sqrt{2}\right)^4\left(-ak_n\cos\left(ak_n\right)+\sin\left(ak_n\right)\right)}{k_n^2{\varepsilon_s}^2}-\frac{R_p Aq^2\left(\sigma\sqrt{2}\right)^3\left(-1+\cos\left(ak_n\right)\right)}{k_n^1{\varepsilon_s}^2} \quad (37)$$

$$C_{6n}=\frac{q^2\left(\sigma\sqrt{2}\right)^6 c_c\left(N_p-N_s\right)\left(-1+\cos\left(ak_n\right)\right)}{{\varepsilon_s}^2 k_n^1}\times\left(\left(a_c+2b_c\left(\frac{a-R_p}{\sigma\sqrt{2}}\right)\right)^2-2b_c\right)e^{\left(-a_c\left(\frac{a-R_p}{\sigma\sqrt{2}}\right)-b_c\left(\frac{a-R_p}{\sigma\sqrt{2}}\right)^2\right)} \quad (38)$$

$$C_{7n}=\frac{q\left(\sigma\sqrt{2}\right)^2\left(1-\cos k_n a\right)}{{\varepsilon_s}^2 k_n}\left[c_c\left(N_p-N_s\right)e^{\left[-\left(a_c\left(\frac{-R_p}{\sqrt{2}\sigma}\right)+b_c\left(\frac{-R_p}{\sqrt{2}\sigma}\right)^2\right)\right]}+\frac{N_s}{2}\left(\frac{-R_p}{\sqrt{2}\sigma}\right)^2-\frac{R\tau_p}{a}\left(\frac{-R_p}{\sqrt{2}\sigma}\right)^2+\frac{\Phi_o\tau_n e^{\left(-\alpha R_p\right)}e^{\left(\alpha R_p\right)}}{\alpha\left(\sigma\sqrt{2}\right)^2}\right]-\frac{\left(V_{bi}-V_{gs}-V_{op}\right)\left(1-\cos k_n a\right)}{k_n} \quad (39)$$

$$M_n=\frac{2ak_n-\sin\left(2ak_n\right)}{4k_n} \quad (40)$$

Thus, the resultant expression $\phi(x,y)$ can be obtained by using the expressions of $\varphi_{1D}(y)$ and $\varphi_{2D}(x,y)$ from Eq. (20) and Eq. (28) in Eq. (16), respectively.

Note that Eq. (28) is an infinite series and hence impossible to use for computation of the values of $\varphi_{2D}(x,y)$ by taking all the terms into consideration. It may be mentioned that any hyperbolic sine function, say $\sinh(z)$, decreases exponentially with the increase in z. Thus, both $\sin\left(k_n(L-x)\right)$ and $\sin\left(k_n L\right)$ in Eq. (28) decreases very rapidly with the increase in n since k_n is increased with n. Further, it may be verified that both A_n and B_n are also decreased with the increase in n. Therefore, it may be a quite reasonable assumption to consider only the fundamental term for $n=1$ of the series to approximately express $\phi(x,y)$ as

$$\phi(x,y)\approx\varphi_{1D}(y)+\frac{\sin(k_1 y)}{\sinh(k_1 L)}\left\{A_1\sinh[k_1(L-x)]+B_1\sinh(k_1 x)\right\} \quad (41)$$

Where k_1, A_1, and B_1 can be determined by using $n=1$ in Eqs. (29-31) respectively.

2. Modeling of Threshold Voltage

The threshold voltage, V_{th}, of a short channel optically biased MESFET can be obtained as [40],

$$V_{th}=V_{tho}-\sec\left(\frac{k_1 L}{2}\right)A_1 \quad (42)$$

where k_1 and A_1 are obtained from Eq. (29) and Eq. (30) with $n=1$, respectively, and V_{tho} is the threshold voltage of the long-channel MESFET which can be obtained as [40]:

$$V_{tho}=V_{bi}-V_{po}-V_{op} \quad (43)$$

where V_{po} is the pinch-off voltage defined as [41],

$$V_{po}=\frac{q}{\varepsilon_s}\int_0^a N_D(y)\,y\,dy \quad (44)$$

$$V_{po}=\frac{q\left[C_1+\left(N_p-N_s\right)\sigma\sqrt{2}\left(C_2+C_3+C_4\right)\right]}{\varepsilon_s} \quad (45)$$

$$C_1=\frac{N_s a^2}{2}-\frac{R\tau_p a}{2}+\left[\frac{\left(1-\left(1+a\alpha\right)e^{(-a\alpha)}\right)\Phi_o\tau_n}{\alpha}\right] \quad (46)$$

$$C_2 = -\sigma\sqrt{2}c_c\left[e^{\left(-\frac{a_c(a-R_p)}{\sigma\sqrt{2}}-b_c\left(\frac{(a-R_p)}{\sigma\sqrt{2}}\right)^2\right)} - e^{\left(-\frac{a_c(-R_p)}{\sigma\sqrt{2}}-b_c\left(\frac{(-R_p)}{\sigma\sqrt{2}}\right)^2\right)}\right] \quad (47)$$

$$C_3 = c_c(a-R_p)\left(a_c + 2b_c\frac{(a-R_p)}{\sigma\sqrt{2}}\right)e^{\left(-\frac{a_c(a-R_p)}{\sigma\sqrt{2}}-b_c\left(\frac{(a-R_p)}{\sigma\sqrt{2}}\right)^2\right)}$$

$$-c_c(-R_p)\left(a_c + 2b_c\frac{(-R_p)}{\sigma\sqrt{2}}\right)e^{\left(-\frac{a_c(-R_p)}{\sigma\sqrt{2}}-b_c\left(\frac{(-R_p)}{\sigma\sqrt{2}}\right)^2\right)} \quad (48)$$

$$C_4 = -R_p c_c\left[\left(a_c + 2b_c\frac{(a-R_p)}{\sigma\sqrt{2}}\right)e^{\left(-\frac{a_c(a-R_p)}{\sigma\sqrt{2}}-b_c\left(\frac{(a-R_p)}{\sigma\sqrt{2}}\right)^2\right)}\right.$$

$$\left.-\left(a_c + 2b_c\frac{(-R_p)}{\sigma\sqrt{2}}\right)e^{\left(-\frac{a_c(-R_p)}{\sigma\sqrt{2}}-b_c\left(\frac{(-R_p)}{\sigma\sqrt{2}}\right)^2\right)}\right] \quad (49)$$

IV. Outline of ATLAS™ Simulation

ATLAS™ device simulation software has been used to obtain the numerical simulation data for the validation of our proposed model. The device has been simulated by assuming ITO (with work function=4.7 eV [42], refractive index=1.96 [43]) as the gate electrode. The transmission property of the gate has been set using INTERFACE keyword in the ATLAS program. The drift-diffusion (DD) model available in ATLAS library has been used. To turn on the optical recombination model, the OPTR keyword on the MODELS statement has been turned ON. Other models used for the recombination are SRH (Shockley-Read-Hall recombination), and AUGER (Auger recombination). The mobility models used are CONMOB (concentration field dependent mobility model) and FLDMOB (electric field dependent mobility model).

V. Results and Discussion

In this section, we will compare our model results with those obtained by using the commercially available 2D device simulator ATLAS™. The values of the parameters used for computation of the model results are: a=0.2 μm, V_{gs}=0.1 V, R_p=0.06 μm, V_{bi}=0.67 V, σ=0.05 μm, N_p=1×10^{23} m^{-3}, N_s=1×10^{21} m^{-3}, τ_n=10^{-6} s, τ_n=10^{-8} s, α=10^6/m, λ=8700 Å and T_m=0.9.

First of all, we have compared $F_1(Y) = c_c\{(a_c + 2b_c\beta Y)^2 - 2b_c\}\exp\left[-\{a_c\beta Y + b_c Y^2\}\right]$ of Eq. (4) with $F_2(Y) = F(\sigma\sqrt{2}\,Y + R_p) = \exp(-Y^2)$ of Eq. (3) in Fig. 2 for showing the validity of the Eq. (4) with $Y = \frac{y-R_p}{\sigma\sqrt{2}}$. It is observed that the two curves are well-matched for $-2.2 \le Y \le 2.2$. Since, the value of the functions fall by nearly two order of magnitude for $-2.2 \le Y \le 2.2$, the approximated function $F_2(y)$ can considered to be valid for most of the practical applications.

Fig. 3 shows the variation of channel potential with the gate length (L) in dark and illuminated conditions for different gate to source voltages (V_{gs}). It can be seen that, for a given gate length, the source-channel potential barrier is reduced due to the incident optical radiation on the device. This is due to the fact that the photovoltage developed across the junction due to illumination forward biases the Schottky gate–channel junction and thereby decreasing the source-channel barrier potential. This implies that the height of the depletion region below the gate is decreased with the increase in the level of incident illumination on the device.

The channel potential variation as a function of channel length (L) has been shown in Fig. 4 for different values of projected straggle σ. It is observed that source-channel barrier height is decreased with the

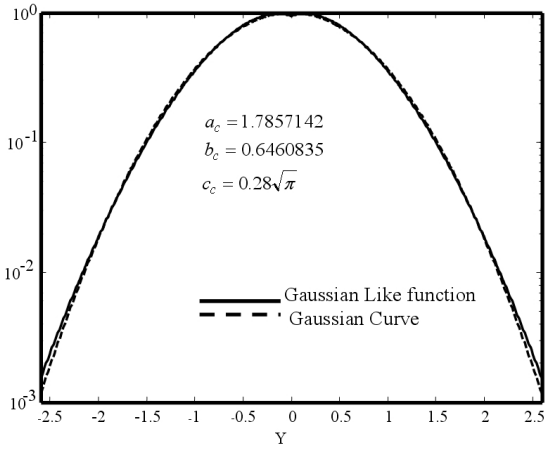

Fig. 2. Comparison of Gaussian and New Gaussian like function curves.

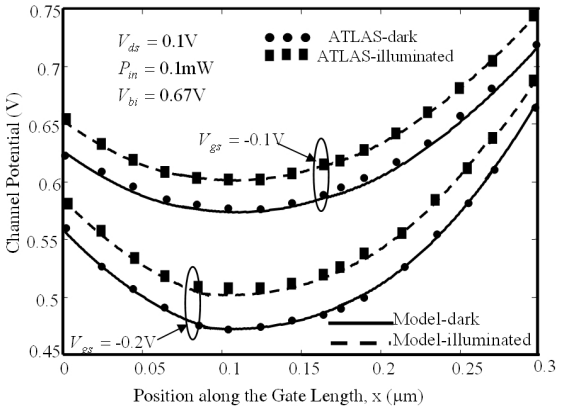

Fig. 3. Variation of channel potential along the channel length for different gate to source voltages (V_{gs}) in dark and illuminated conditions.

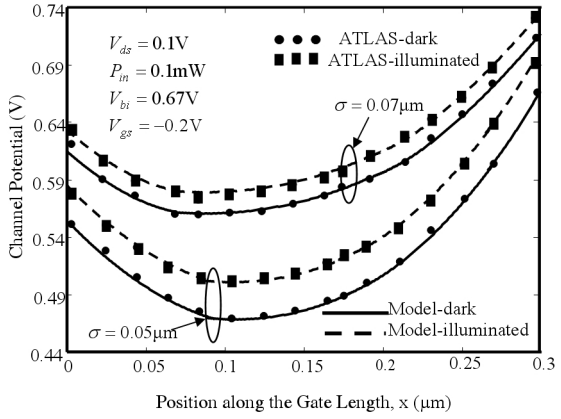

Fig. 4. Variation of channel potential along the channel length for different standard deviation (σ) in dark and illuminated conditions.

increase in the value of σ due to the increase in the average implanted ion density in the active channel region of the MESFET with the increase in σ of the profile for a constant peak doping N_p.

Fig. 5 shows the threshold voltage (V_{th}) variation with gate length for dark and illuminated conditions. It has been observed that, for gate length less than 0.2 μm, drain induced barrier lowering (DIBL) effect becomes prominent which, in turn, reduces the threshold voltage of the device. It is also found that the threshold voltage under illuminated condition is smaller that that obtained under the dark condition of the device. This is due to the development of photovoltage at the Schottky gate owing to the incident optical radiation which makes the junction forward biased.

Variation of the threshold voltage (V_{th}) with incident optical power (P_{in}) on the device is shown in Fig. 6. The figure shows that the threshold voltage is decreased with the increase in the incident optical power. The abrupt change in threshold voltage at $0.1\,\mathrm{mW}$ is due to the fact that the developed photovoltage is too small to make a change in the device characteristics below the mentioned power level. Once the incident optical power is increased beyond the above level, the photo-generated carriers become sufficient in numbers to develop a significant amount of photovoltage which forward biases the gate-channel junction and reduces the threshold voltage of the device.

Fig. 7 shows the variation of threshold voltage (V_{th}) with gate length (L) under illuminated condition of the

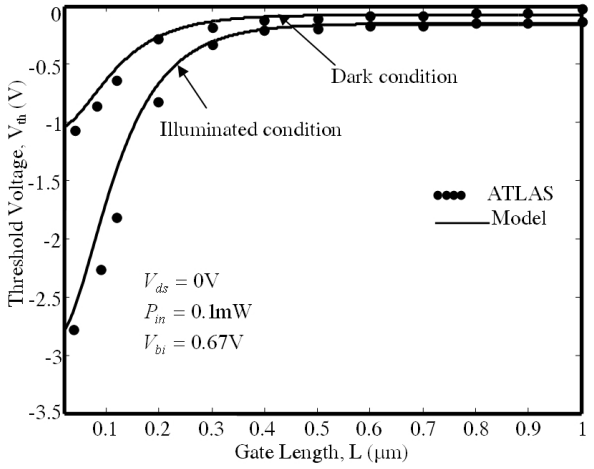

Fig. 5. Threshold voltage (V_{th}) variation with gate length (L) for dark and illuminated conditions.

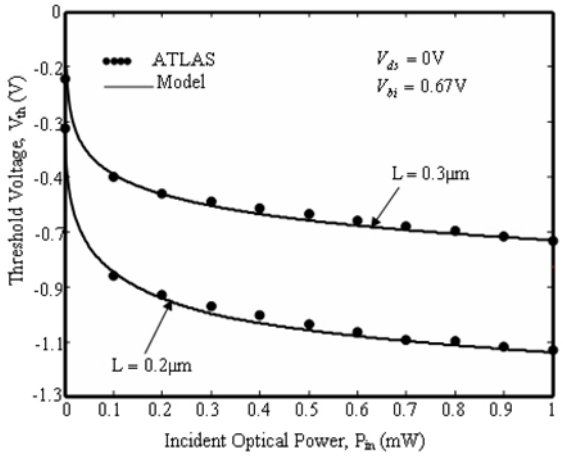

Fig. 6. Variation of threshold voltage (V_{th}) with incident optical power (P_{in}) for different gate lengths (L).

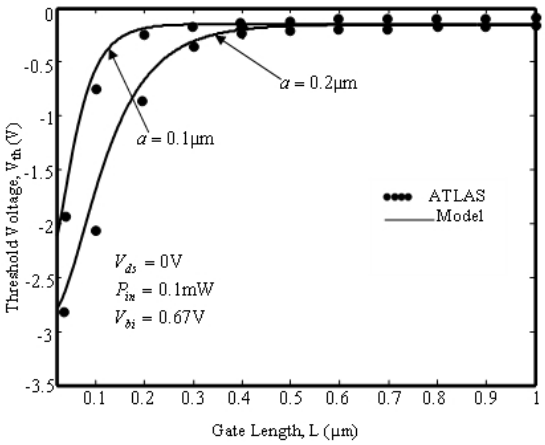

Fig. 7. Variation of threshold voltage (V_{th}) with gate length (L) for different channel thickness.

device for different channel thickness (a). It is observed that threshold voltage degradation due to short-channel effect can be optimized by reducing the channel thickness.

VI. CONCLUSIONS

In this paper, a 2D channel potential has been modeled for fully depleted optically biased GaAs MESFET device with a Gaussian-like doping profile in the vertical direction. The 2D potential distribution has been derived by solving the 2D Poisson's equation using the separation of variable technique. Optical radiation dependent threshold voltage expression has also been derived and compared with dark condition. The observed threshold voltage degradation due to short-channel effects can be minimized by reducing channel thickness of a GaAs MESFET. The proposed model results are found to be well-matched with the ATLAS™ simulation data.

REFERENCES

[1] S. Sabat, L.D.S. Coelho, A. Abraham, "MESFET DC model parameter extraction using quantum particle swarm optimization," *Microelectronics Reliability* Vol.49, No. pp.660-666, Apr., 2009.

[2] I. J.Bahl, "2.8 GHz 8-W Power Amplifier MMIC Developed Using MSAG MESFET Technology," *IEEE Microwave and Wireless Components Lett.* Vol.18, No.1, pp.52-54, Jan., 2008.

[3] B. Y. Martynov, E. V. Pogorelova, "Influence of Substrate Purity on MESFET Parameters," *Proceedings of 17th International Crimean Conference on Microwave & Telecommunication Technology*, pp.121-122, Sep., 2007.

[4] I. J. Bahl, D. Conway, "L and S-Band Compact Octave Bandwidth 4-bit MMIC Phase Shifters," *IEEE Trans. Microwave Theory Tech.* Vol.56, No.2 , pp.293-299, Feb., 2008.

[5] V. Eveloy, H. Yu-Chul, "The Effect of Electrostatic Discharge on Electrical Overstress Susceptibility in a Gallium Arsenide MESFET-Based Device," *IEEE Trans. on Dev. and Mater. Reliability* Vol.7, No.1, pp.200-208, Mar., 2007.

[6] J. A Torres, J. C. Freire, "Monolithic transistor SPST switch for L-band," *IEEE Trans. Microwave Theory Tech.* Vol.50, No.1, pp.51-56, Jan., 2002.

[7] F. Ellinger, R. Vogt, "Ultra compact, low loss, varactor tuned phase shifter MMIC at C-band," *IEEE Microwave and Wireless Components Lett.* Vol.11, No.3, pp.104-105, Mar., 2001.

[8] C. H. Lee, S. Han, "A low phase noise X-band MMIC GaAs MESFET VCO," *IEEE Microwave and Guided Wave Lett.* Vol.10, No.8, pp.325-327, Aug., 2000.

[9] T. L. Nguyen, A. P. Freundorfer, "A balanced distributed preamplifier using MMIC GaAs MESFET technology," *IEEE Photonics Tech. Lett.* Vol.9, No.4, pp.499-501, Apr., 1997.

[10] J. M. Zamanillo, J. Portilla, C. Navarro, C. Pérez-Vega., "Optical Ports: Next generation of MMIC control devices," *Proceedings of 35th European Microwave Conference (EuMC),* pp.1391-1394, Oct., 2005.

[11] A. P. Freundorfer, D. H. Choi, "Adaptive transversal preamplifier for high speed lightwave systems," *IEEE Microwave and Wireless Components Lett.* Vol.11, No.7, pp.293-295, July, 2001.

[12] J. Rodriguez-Tellez, K. A. Mezheg, N T. AIi, T. Fernandei, A. Mediavilla, A. Tazon, C. Navarro, "Optically controlled 2.4GHz MMIC Amplifier," *Proceedings of 10th International Conference on Electronics, Circuits & Systems (ICECS),* pp.970-973, Dec., 2003.

[13] M. A. Alsunaidi, "Optoelectronic conversion of short pulses in sub micrometer GaAs active devices,"

Opt. Quant. Electronics Vol.40, No.9, pp.685-694, July, 2008.

[14] J. M. Zamanillo, J. Portilla, C. Navarro, C. Pérez-Vega, "Optoelectronic control of a MMIC VCO at Ku band," *Proceedings of the 5th WSEAS International Conference on Electronics, Hardware, Wireless and Optical Communications*, pp.138-141, Feb. 2007.

[15] S. Jit, B. B. Pal, "A new Optoelectronic Integrated Device for Light-Amplifying Optical Switch (LAOS)," *IEEE Trans. Electron Device* Vol.48, No.12, pp.2732-2739, Dec., 2001.

[16] S. Kawasaki, H. Shiomi, "A novel FET model including an illumination intensity parameter for simulation of optically controlled millimeter-wave oscillators," *IEEE Trans. Microwave Theory Tech.* Vol.46, No.6, pp.820-828, June, 1998.

[17] I. W.Smith, R. C. Sharp, "Demonstration of photonically controlled GaAs digital/MMIC for RF optical links," *IEEE Trans. Microwave Theory Tech*, Vol.45, No.1, pp.15-22, Jan., 1997.

[18] S. Bose, M. Gupta, R.S. Gupta, "Cut-off frequency and optimum noise figure of GaAs optically controlled FET," *Microwave Opt. Technol. Lett.* Vol.26, No.5, pp.279-282, Sep., 2000.

[19] S. Bose, Adarsh, R.S. Gupta, "Unilateral power gain of optically biased GaAs MESFET," *Appl Microwave Wireless* , Vol.13, No.8, pp.68-77, Aug., 2001.

[20] Madjar, A. Paolella, P. R. Herczfeld, "Analytical model for optically generated currents in GaAs MESFETs," *IEEE Trans. Microwave Theory Tech.* Vol.40, No.8, pp.1681-1691, Aug., 1992.

[21] P. Chakrabarti, A. Gupta, N. A. Khan, "An Analytical Model of GaAs OPFET," *Solid-State Electronics* Vol.39, No.10, pp.1481-1490, Oct., 1996.

[22] A. A. De Salles, Optical control of GaAs MESFETs, *IEEE Trans. Microwave Theory Tech.* Vol.31, No.10, pp.812-820, Oct., 1983.

[23] S. Mishra, V. K. Singh, B. B. Pal, "Effect of radiation and surface recombination on the characteristics of an ion -implanted GaAs MESFET," *IEEE Trans. Electron Device* Vol.37, No.1, pp.2-10, Jan., 1990.

[24] S. Bose, Adarsh, Ritesh Gupta, Mridula Gupta and R S Gupta "Model for optically biased Short channel GaAs MESFET," *Microwave Opt. Technol. Lett.* Vol.32, No.2, pp.138-142, Jan., 2002.

[25] S. Bose, M. Gupta, R.S. Gupta, "I_d -V_d characterristics of optically biased short channel GaAs MESFET," *Microelectron J* Vol.32, No.3, pp.241-247, Mar., 2001.

[26] P. Calvani, A. Corsaro, "Microwave operation of sub-micrometer gate surface channel MESFETs in polycrystalline diamond," *Microwave Opt. Technol. Lett.* Vol.51, No.11, pp.2786-2788, Nov., 2009.

[27] E. Donkor, F. C. Jain, "An Analytical Two-Dimensional Perturbation Method to Model Submicron GaAs MESFETs," *IEEE Trans. Microwave Theory Tech.* Vol.37, No.9, pp.1484-1487, Sep., 1989.

[28] N. Kato, K. Yamasaki, K. Asai, K. Ohwada, "Electron beam lithography in n+ self-aligned GaAs MESFET fabrication," *IEEE Trans. Electron Device* Vol.30, No.6 , pp.663-668, June, 1983.

[29] P. C. Chao, P. M. Smith, S. Wanuga, W. H. Perkins, E. D. Wolf, "Channel length effects in quarter micrometer gate-length GaAs MESFETs," *IEEE Electron Device Lett.* Vol.4, No.9, pp.326-328, Sep., 1983.

[30] C. H. Liu, L. W. Wu, S. J. Chang, J. F. Chen, U. H. Liaw, S. C. Chen, "Ion-implantation technology for improved GaAs MESFETs performance," *J. of Mater. Sci.:Mater in Electronics* Vol.15, No.2, pp.91-93, Feb., 2004.

[31] A. Dasgupta, S. K. Lahiri, "A novel analytical threshold voltage model of MOSFETs with implanted channels," *Int. J. Electronics* Vol.61, No.5, pp.655-669, May, 1986.

[32] ATLAS: Silvaco International 2008.

[33] S. A Bashar "Study of Indium Tin Oxide(ITO) for Novel Optoelectronic Devices," *PhD Thesis, King's College of London*, University of London, 1998.

[34] S.M. Sze, *Physics of semiconductor devices*, second ed., Wiley, New York, 1981.

[35] A. Dasgupta, S. K. Lahiri, "A two-dimensional analytical model of threshold voltages of short-channel MOSFETs with Gaussian-doped channels," *IEEE Trans. Electron Device* Vol.35, No.3, pp.390-392, Mar., 1988.

[36] S. Kabra, H. Kaur, S. Haldar, M. Gupta, R.S. Gupta, "Two-dimensional subthreshold analysis of sub-micron GaN MESFET," *Microelectronics Journal* Vol.38, No.4 pp.547-555, Apr., 2007.

[37] S. Jit, G. Bandhawakar, B. B. Pal, "Analytical

Modeling of a DCFL Inverter Using Normally-off GaAs MESFETs Under Dark and Illuminated Conditions," *Solid-State Electronics* Vol.49, No.4, pp.628-633, Feb., 2005.

[38] K.N. Ratnakumar, J.D. Meindel, "Short channel MOST threshold voltage model," *IEEE J. Solid State Circuits* Vol.17, No.5, pp.937-947, Oct., 1982.

[39] E. Kreyszig, *Advanced Engineering Mathematics*, seventh ed., Wiley, New York, 1993.

[40] S. P. Chin, C. Y. Wu, "A new two dimensional model for the potential distribution of short gate length MESFETs and its application," *IEEE Trans. Electron Device* Vol.39, No.8, pp.1928-1937 Aug., 1992.

[41] Michael Shur, *GaAs devices and circuits*, Plenum Press, New York, 1986.

[42] I. D. Parker, "Carrier tunneling and device characteristics in polymer light-emitting diodes," *J. Appl. Phys*. Vol.75, No.3, pp.1656-1666, Feb., 1994.

[43] J. Szczyrbowski, "A. Dietrich and H. Hoffmann, Optical and Electrical Properties of r.f. Sputtered Indium-Tin Oxide Films," *Phys Stat Sol (a)*, Vol.78, No.1, pp.243-252, July, 1983.

Shweta Tripathi was born in Allahabad district, Uttar Pradesh (UP), India on March 3, 1984. She received the B.Tech. degree in Electronics and Communication Engineering from the Uma Nath Singh Institute of Engineering and Technology, V.B.S. Purvanchal University, UP, India in 2006. Presently, she is pursuing her Ph.D. degree in the Department of Electronics Engineering, Institute of Technology, Banaras Hindu University, India. Her present research interests include modeling and simulation of short channel GaAs MESFETs under dark and illuminated conditions.

S. Jit has earned his B.E. degree from the Department of Electronics and Telecommunication Engineering, Bengal Engineering College, University of Calcutta, West Bengal, in 1993, M.Tech. degree from the Department of Electrical Engineering, Indian Institute of Technology (IIT), Kanpur, India, in 1995, and the Ph.D. degree from the Department of Electronics Engineering, Institute of Technology (IT), Banaras Hindu University (BHU), Varanasi, India in 2002. Dr. Jit joined the Department of Electronics Engineering, IT-BHU, Varanasi as Lecturer in 1998 where he has been working as Associate Professor since 2007.

Dr. Jit is the recipient of Visiting Fellowship of the *Indian National Science Academy* (INSA) in 2006. He has worked as *Postdoctoral Research Fellow* in the Optolelctronics Laboratory, Department of Physics and Astronomy, Georgia State University, Atlanta, USA during March-August, 2007. Dr. Jit has published more than 50 papers in various peer reviewed international journals and conference proceedings. His present research interests include modeling and simulation of optically controlled microwave devices and circuits, terahertz photodetectors, short-channel SOI-MESFETs, multiple-gate SOI-MOSFETs, etc. Dr. Jit is the *Fellow* of the *Institution of Electronics and Telecommunication Engineers (IETE)*, India.